Fast Computation of Combustion Phasing and Its Influence on Classifying Random or Deterministic Patterns

Huan Lian[1]
Department of Mechanical Engineering,
University of Michigan,
Ann Arbor, MI 48109
e-mail: hlian@umich.edu

Jason Martz
Department of Mechanical Engineering,
University of Michigan,
Ann Arbor, MI 48109

Niket Prakash
Department of Mechanical Engineering,
University of Michigan,
Ann Arbor, MI 48109

Anna Stefanopoulou
Department of Mechanical Engineering,
University of Michigan,
Ann Arbor, MI 48109

The classification between a sequence of highly variable combustion events that have an underlying deterministic pattern and a sequence of combustion events with similar level of variability but random characteristics is important for control of combustion phasing. In the case of high cyclic variation (CV) with underlying deterministic patterns, it is possible to apply closed-loop combustion control on a cyclic-basis with a fixed mean value, such as injection timing in homogeneous charge compression ignition (HCCI) or spark timing in spark ignition (SI) applications, to contract the CV. In the case of a random distribution, the high CV can be avoided by shifting operating conditions away from the unstable region via advancing or retarding the injection timing or the spark timing in the mean-sense. Therefore, the focus of this paper is on the various methods of computing CA50 for analyzing and classifying cycle-to-cycle variability. The assumptions made to establish fast and possibly online methods can alter the distribution of the calculated parameters from cycle-to-cycle, possibly leading to incorrect pattern interpretation and improper control action. Finally, we apply a statistical technique named "permutation entropy" for the first time on classifying combustion patterns in HCCI and SI engine for varying operating conditions. Then, the various fast methods for computing CA50 feed the two statistical methods, permutation and the Shannon entropy, and their differences and similarities are highlighted. [DOI: 10.1115/1.4033469]

1 Introduction

Control of combustion process on a cycle-to-cycle basis can improve fuel economy and emission performance. The characteristics of combustion process represented by combustion phasing could be random [1] or deterministic [2,3] and would lead to a different control strategy aiming to contract the CV. In the case of high CV with underlying deterministic patterns, it is possible to apply closed-loop combustion control of certain variable on a cycle-basis with a fixed mean value, such as injection timing in HCCI engine or spark timing in SI engine, to contract the CV. In the case of a random distribution, the high CV should be avoided by shifting operating conditions via advancing or retarding the injection timing or the spark timing in the mean-sense.

Real time heat release can be used with statistical methods for online quantification of combustion process variations as random or deterministic. However, errors within these fast heat release (fHR) analyses can bias sequence statistics and lead to the incorrect classification of combustion variations as random or deterministic, potentially leading to improper control action. In the current work, we compare the influence of several fHR methods on the statistics of deterministic, high CV HCCI combustion and SI combustion, where the CV is random in nature.

The paper is organized as follows: In Sec. 2, three fast computational methods for the determination of combustion phasing are briefly described. In Sec. 3, CV is quantified with return maps, the modified Shannon entropy, and symbol statistics. The impact of each combustion phasing estimation method on the quantification of CV is assessed through comparison with the baseline detailed heat release (dHR) analysis [4]. Section 4 introduces a diagnostic technique based on the permutation entropy to classify if SI and HCCI combustion process are deterministic or random, which is necessary for choosing the optimal control strategy. Comparisons with modified Shannon entropy are also included. Figure 1 summarizes the scope of the current work.

2 Estimation of Combustion Phasing

Three fast combustion phasing estimation methods have been evaluated for HCCI and SI combustion phasing: fast, single-zone heat release with a constant ratio of specific heats [2], Rasseweiler and Withrow's (R&W) method based on the assumption of isentropic compression and expansion [2], and Marvin's graphic method [6]. The methods were evaluated offline against dHR analysis which estimates burned gas properties with chemical equilibrium and a routine for the prediction of trapped residual mass [5].

2.1 Experimental Setup. SI and HCCI combustion experiments were performed in a prototype modified four-cylinder 2.0 L SI engine, based on the GM Ecotec, running on Tier-II certification gasoline fuel. The compression ratio was 11.7, the bore and stroke were 88 mm, and the connecting rod length was 146 mm. The engine was designed for running multiple modes of combustion, such as an HCCI, spark assisted compression ignition (SACI), and SI. The important features of the engine were dual-lift valvetrain with dual-independent cam phasers, external exhaust gas recirculation (eEGR), spray-guided direct and port fuel injection, and in-cylinder pressure sensing. The data presented here for SI combustion were operated close to stoichiometry, with direct injection and with low cam lift intake and exhaust profile. Negative valve overlap was utilized to trap up to approximately 40% internal residual, while a high-pressure EGR system provides cooled external residual gas [7,8]. For HCCI combustion, the data were taken from experiments at constant speed of

[1]Corresponding author.

Contributed by the IC Engine Division of ASME for publication in the JOURNAL OF ENGINEERING FOR GAS TURBINES AND POWER. Manuscript received January 4, 2016; final manuscript received April 8, 2016; published online May 17, 2016. Editor: David Wisler.

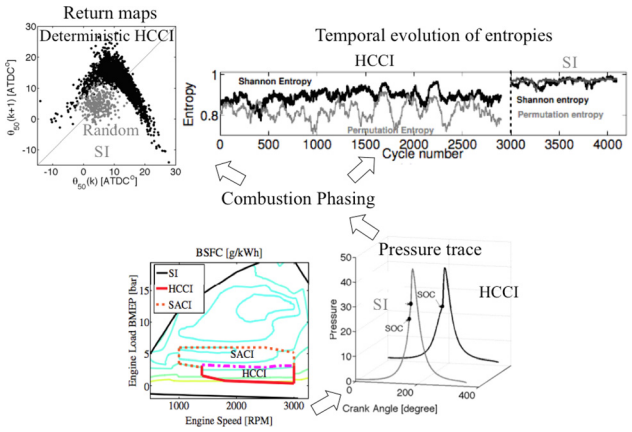

Fig. 1 Scope of the current work (engine map from Ref. [5])

2000 rpm, with fuel injection at 60 deg after top dead center with negative valve overlapping. The chosen condition was diluted and lean with approximately 50% residual gas and air–fuel equivalence ratio of 1.3–1.4 [9].

2.2 Marvin's Method. Marvin [6] proposed a graphical method with a logarithmic P–V diagram based on the assumption that both compression and expansion processes follow a polytropic relation

$$PV^{\gamma} = \text{constant} \tag{1}$$

Marvin's method is illustrated in Fig. 2. Constant volume combustion was assumed to follow the polytropic compression process with the pressure rise shown between points b and d. The mass fraction burned at point c on the line b–d can be estimated as

$$x_b = \frac{P_c - P_b}{P_d - P_c} \tag{2}$$

By drawing a line $c - c'$ from point c parallel to the polytropic compression slope that intersects with the actual P–V diagram at c', a combination of in-cylinder pressure and volume is defined

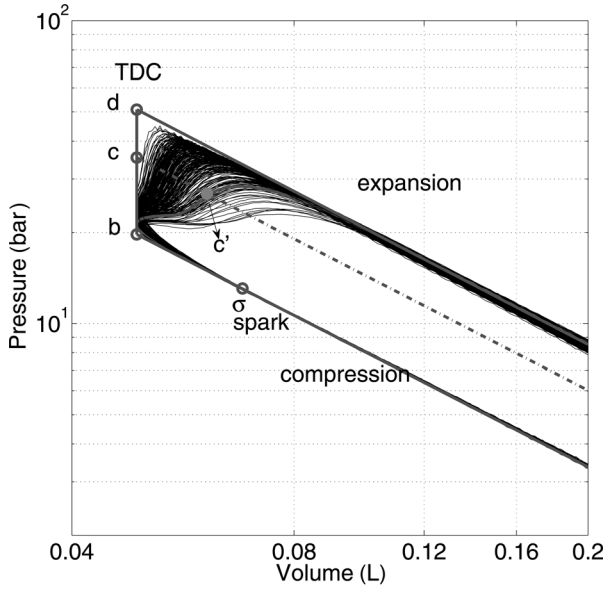

Fig. 2 Marvin's graphical method for estimating combustion phasing of SI combustion, with 42% internal EGR fraction, spark timing 38 deg bTDC, 298 cycles

from the intersection point. The corresponding combustion phasing crank angle can be uniquely calculated from the combination of pressure and volume.

A natural question of this technique is the resolution in defining the intersection point and combustion phasing calculation. We have found that 1/10 crank angle is a reasonable measurement resolution for SI combustion applications, which has been adopted for all the results in the current work. In the case with poor measurement resolution, it is recommended to interpolate the pressure data with a cubic interpolation method to ensure estimation accuracy.

2.3 R&W Method. Another well-known method to estimate combustion phasing was proposed by Rassweiler and Withrow [10], who correlated pressure rise with flame photographs. The analysis assumes that unburned gas with a volume of V_u has been compressed polytropically through the expansion of the charge as it is consumed by the flame front, thus the unburned gas volume $V_{u,\sigma}$ at the start of combustion can be expressed as

$$V_{u,\sigma} = V_u(P/P_\sigma)^{1/n} \tag{3}$$

where P is the crank-angle-resolved in-cylinder pressure, and P_σ is the pressure at the start of combustion, defined as the time of spark timing for SI and intake valve closing (IVC) for HCCI combustion.

Similarly, the burnt gas volume $V_{b,f}$ at the end of combustion (EOC) can be expressed in Eq. (4), where the EOC is arbitrarily defined. In the current work on SI combustion, we define the EOC around the crank angle where the P–V diagram converges to the polytropic expansion phase as shown in Fig. 2. For HCCI combustion, it is difficult to identify the crank angle where the logarithmic P–V diagram converges to the polytropic expansion phase, due to the presence of slow-burning cycles. The EOC is defined approximately 30 deg after top dead center, where combustion ends in most of the cycles. It should be noted that the arbitrary choice of the EOC is the major factor responsible for the inaccuracy of this method

$$V_{b,f} = V_b(P/P_f)^{1/n} \tag{4}$$

The mass fraction burned x_b can be approximated with the unburned gas volume consumed by the flame front as

$$x_b = 1 - \frac{V_{u,\sigma}}{V_\sigma} \tag{5}$$

Combining Eqs. (3) and (5) and considering volume conservation $V = V_u + V_b$, the mass fraction burnt x_b is then derived as

$$x_b = \frac{P^{1/n}V - P_\sigma^{1/n}V_\sigma}{P_f^{1/n}V_f - P_\sigma^{1/n}V_\sigma} \tag{6}$$

The polytropic exponent n has been used as an averaged value of compression and expansion processes.

The combustion phasing crank angle is calculated from the interpolation of the mass fraction burned x_b, with a resolution of 0.1 deg crank angle.

2.4 fHR. The logarithmic P–V diagram provides a good representation of engine work but cannot infer details of the combustion process to directly relate the pressure rise due to the chemical energy released. While dHR analysis based on the first law of thermodynamics includes subroutines for estimating burned gas properties with chemical equilibrium and prediction of the trapped residual mass, these subroutines are time-consuming and inapplicable for online diagnostic purposes. Alternatively, a simplified fHR method that has been widely applied [2] is used here. The

fHR analysis is based on the assumption of a single-zone combustion chamber and a fixed ratio of specific heats for gas properties.

The energy equation based on the first law of thermodynamics can be expressed as follows for a closed system to evaluate its efficiency during high CV conditions:

$$\frac{dQ_{\text{ch}}}{d\theta} = \frac{m_c c_v dT}{d\theta} + P\frac{dV}{d\theta} + \frac{dQ_{\text{ht}}}{d\theta} \tag{7}$$

based on the assumption of ideal gas law

$$PV = m\frac{\overline{R}}{M}T \tag{8}$$

Introducing the differential from the ideal gas law into the energy equation yields

$$\frac{dQ_n}{d\theta} = \frac{dQ_{\text{ch}}}{d\theta} - \frac{dQ_{\text{ht}}}{d\theta} = \frac{\gamma}{\gamma - 1}P\frac{dV}{d\theta} + \frac{1}{\gamma - 1}V\frac{dP}{d\theta} \tag{9}$$

The apparent heat release is calculated by solving Eq. (9), while gamma is assumed to be constant (1.35). Equation (9) was evaluated from the start to end of combustion (SOC and EOC, respectively) to determine the net rate of heat release. SOC was defined as the crank angle of IVC for HCCI and the crank angle of spark for SI. EOC was defined as 30 deg after top dead center, where combustion ends in most cycles. The mass fraction burned (x_b) was defined by normalizing the cumulative heat release from SOC to a given crank angle by the net cumulative heat release determined from SOC to EOC. The corresponding combustion phasing is then defined proportional to the mass fraction burned. The initial condition of pressure and volume for each cycle is defined slightly before the SOC from the experimental pressure measurement. Although the residual mass is not considered in this case, the initial condition is updated each cycle to reflect the variation of in-cylinder charge. The coupled equations and their convergence have been studied for an HCCI application in our previous work [11].

While the choice of EOC affects the combustion phasing calculation (CA50), this choice did not affect the HCCI and SI symbol statistics for slow-burning or misfiring cycles or the quantification of random or deterministic patterns discussed in Sec. 3. Due to the equally probable coarse binning approach, this approach lumps very slow-burning and misfiring cycles into a single bin.

Applying the three methods on pressure data from SI combustion, the CA50 calculated from each method is shown in Fig. 3. It is shown in Figs. 3(*a*) and 3(*b*) that all the three fast computation methods perform well for SI combustion with small discrepancies relative to the baseline detailed heat release analysis, labeled as dHR. The CA50 calculation for HCCI combustion is shown in Fig. 4. Deviations from baseline are observed for all of the three fast computation methods. However, the inaccuracies of these three methods in the estimation of SI combustion phasing were found mostly for slow-burning cycles. CA50 computations were performed on a 2 GHz Intel Core i7 with 8 GB memory, with calculation times (per cycle) within 10 ms for the three methods.

In summary, the fHR and R&W methods are accurate for rapid burning HCCI combustion cycles but could result in discrepancies in late burning cycles. This is due to the fact that both methods involve an arbitrarily defined EOC, which contributes to most of the inaccuracy in phasing estimations for the late burning cycles. Marvin's method could result in noticeable deviation due to the constant volume assumption and limited resolution when determining the intersection point.

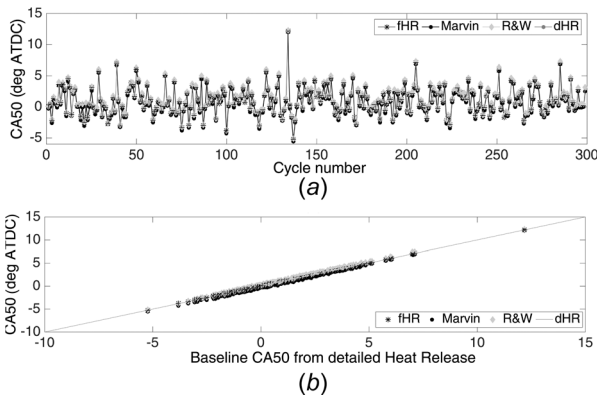

Fig. 3 CA50 calculation of SI combustion with 42% internal EGR fraction, spark timing 38 deg bTDC: (*a*) scatter plot and (*b*) relationship with the baseline CA50 from dHR. Detailed heat release is noted as dHR and fast heat release is noted as fHR. Marvin's method is noted as Marvin, and Rasseweiler and Withrow's method is noted as R&W.

3 Determinism Versus Randomness in CV

The cyclic dispersion of SI and HCCI combustion was quantified with return maps, modified Shannon Entropies, and symbol sequence statistics [9] of the estimated combustion phasing parameters. These techniques help to quantify the influence of deterministic patterns in the seemingly random events. A brief summary of the three techniques is included for clarification purposes. A detailed description of these techniques can be found in Ref. [3]. In this section, we investigate if the skewness of the fast methods described earlier could also affect the entropy of the combustion phasing for both deterministic HCCI and random SI combustion.

A return map qualitatively shows the relationship of two consecutive cycles of a specific cycle-dependent combustion feature. The modified Shannon entropy [3] is a quantitative measurement of the randomness of a given time series sequence. It shows the temporal correlation in time series data when discretized into symbols with a specific sequence division N and length L and is defined as

$$H_s = -\frac{1}{\log n_{\text{seq}}}\sum_k p_k \log p_k \tag{10}$$

where p_k is the probability of observing a sequence k, and n_{seq} is the number of different sequences observed in the time series. The entropy equaling 1 ($H_s = 1$) represents a random process, while $H_s < 1$ shows the presence of deterministic patterns. In practice, the modified Shannon entropy can be used to: (a) quantify the randomness in time series data and (b) optimize symbol sequence parameters N and L, with the best representation of temporal correlation occurring in the engine cycles. The symbol sequence

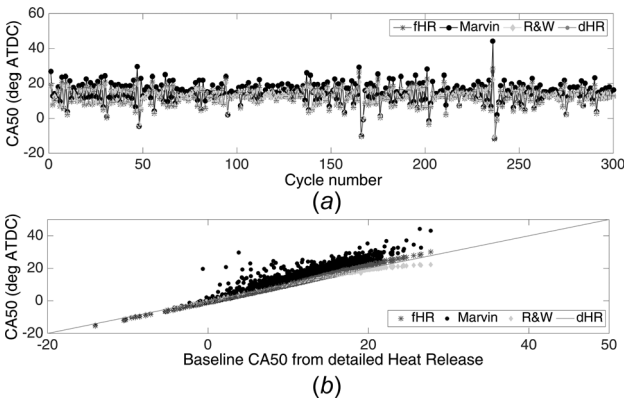

Fig. 4 CA50 calculation of HCCI combustion: (*a*) scatter plot and (*b*) relationship with the baseline CA50 from dHR

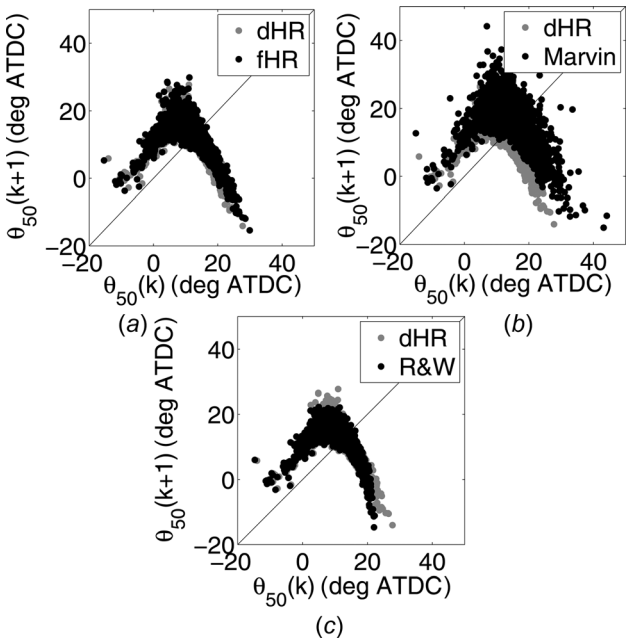

Fig. 5 Return map of CA50 of high CV HCCI combustion: (*a*) detailed heat release (noted as dHR in gray dots) versus fast heat release (noted as fHR, in black dots), (*b*) detailed heat release (noted as dHR in gray dots) versus Marvin's method (noted as Marvin, in black dots), and (*c*) detailed heat release (noted as dHR in gray dots) versus Rasseweiler and Withrow's method (noted as R&W, in black dots)

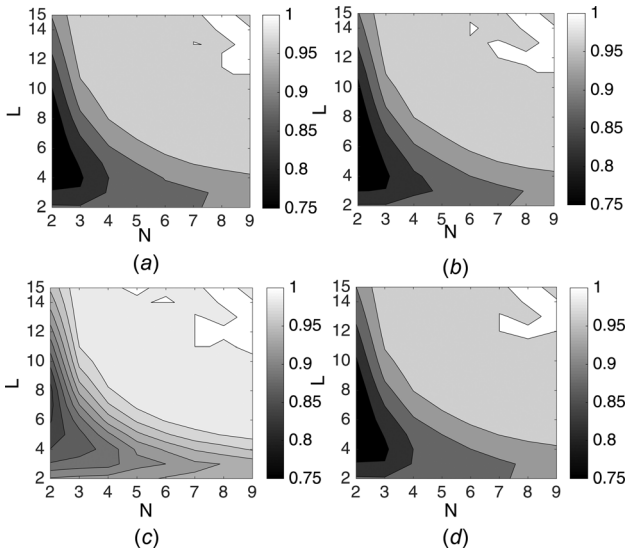

Fig. 6 The modified Shannon entropy of CA50 of high CV HCCI combustion: (*a*) dHR, (*b*) fHR, (*c*) Marvin's method, and (*d*) R&W method

histogram describes the probability of the occurrence of a specific sequence and hence could point to a deterministic mechanism causing this sequence.

3.1 Impact of Combustion Phasing Estimation on the Deterministic Patterns. To examine the impact of the combustion phasing estimation on quantifying deterministic patterns, we used previously published HCCI data [9]. The CA50 of HCCI combustion has been used to examine the sensitivity of the quantification of CV to processing method. Figure 5 is the return map of CA50 calculated from various fast methods superimposed onto the baseline CA50 calculated with the dHR. Oscillations between early and later cycles are observed, representing the presence of nonrandomness for each of the three fast computation methods. The fHR and R&W method had negligible impact on the return map, while Marvin's method distorts the map slightly.

The modified Shannon entropy of CA50 from dHR is shown in Fig. 6(*a*) as the baseline, with the fHR, Marvin's method, and R&W method shown in Figs. 6(*b*), 6(*c*), and 6(*d*), respectively. The minimum Shannon entropy of the baseline case is around 0.75, with each of the three fast processing methods resulting in a similar value, suggesting that the deterministic dynamic behavior could be captured by either method. However, Marvin's method shows a decrease in the magnitude in the modified Shannon entropy with various combinations of partition number N and sequence length L, consistent with the deviation observed in the return maps in Fig. 5.

The symbol statistics of CA50 are shown in Fig. 7 for the three fast computation method with baseline dHR plotted in gray. Sequence partition number N and sequence length L are defined as 5 and 3, consistent with the approach of our previous work [12]. Such combination yields a magnitude of 0.85 for the modified Shannon entropy, but it is not the lowest value for all of the combinations. Any of the three methods captures certain sequences (for example, 041, 410, 141, and 320) with higher frequency, which suggests the undergoing deterministic dynamics induced by the recirculated residual gas [9]. Despite the discrepancies in estimating CA50 with Marvin's method, the sequences are identified in symbol statistics (Fig. 7(*b*)). This is due to the coarse binning approach of symbol sequencing that ensures the robustness of this quantification technique.

The return map, modified Shannon entropy, and symbol statistics for 298 cycles at the condition with highest internal EGR rate are plotted in Fig. 8. The scatter-ball-shaped return map in Fig. 8(*a*) qualitatively indicates randomness. The contour of the modified Shannon entropy of CA50 with sequence division $N(N = 2, 3, 9)$ and length $L(L = 2, 3, 15)$ is shown in Fig. 8(*b*), with the minimum magnitude of the modified Shannon entropy around 0.975 which quantitatively shows the combustion phasing of SI combustion to be random. There are no sequences with relative high frequency in the symbol statistics shown in Fig. 8(*c*). Thus, in the SI case presented here, we observe randomly distributed patterns in the CVs. This conclusion is obviously reached for all the methods of computing the CA50, since the variability in SI data we observed did not include slow burns and late combustion.

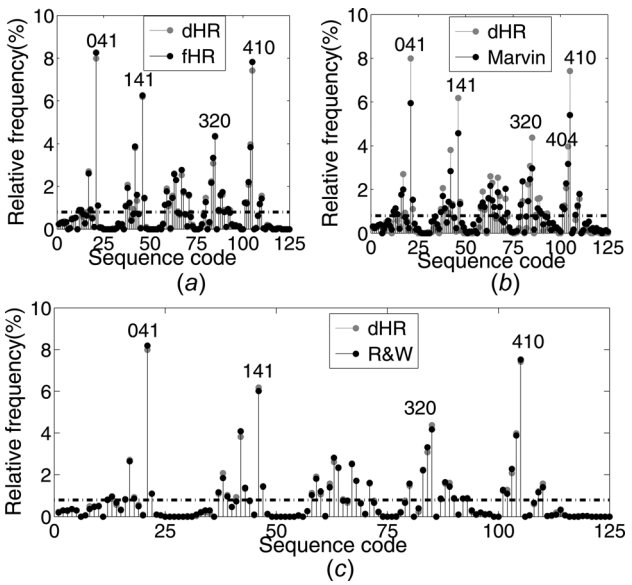

Fig. 7 Symbol statistics of CA50 of high CV HCCI combustion: (*a*) dHR versus fHR, (*b*) dHR versus Marvin's method, and (*c*) dHR versus R&W method

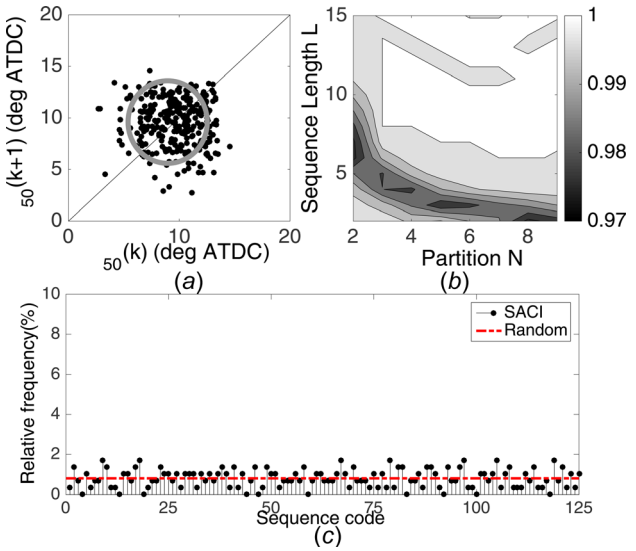

Fig. 8 Quantification of CV in SI combustion with 42% internal EGR fraction, spark timing 38 deg bTDC: (*a*) return map, (*b*) the modified Shannon entropy, and (*c*) symbol statistics

4 Diagnostic of Determinism

To decide if SI and HCCI combustion is deterministic or random and to select the corresponding control strategy, we introduce a diagnostic technique based on the permutation entropy [13,14], which quantifies the rank order pattern of combustion phasing and tracks the temporal development of "determinism" in the time series data. Comparisons with the modified Shannon entropy are made as follows. The theory of permutation is briefly described before discussing an application to HCCI and SI combustion.

4.1 Permutation Entropy. The permutation entropy is an invariant of the rank order pattern in time series data proposed by Bandt and Pompe [13] based on entropy measures and symbolic dynamics. It has been applied to quantify combustion complexity, flame front dynamics [15], and to detect blowout in a lean burn premixed gas-turbine [16]. Symbol statistics rely on coarse binning with the benefit of robustness in the presence of noise. However, this robustness sacrifices the large volume of information contained in the re-representation of the time series data. In order to capture more details, larger partition numbers N and sequence lengths L are needed, but this would result in large number of combinations N^L and would cause difficulties in identifying specific sequences with relatively higher frequency above the random line. Permutation is based on sorting and could provide additional information and work together with Shannon entropy and symbol statistics to examine if the time series data are deterministic or random.

Permutation entropy of the time series data could provide tracking of rank order patterns. Given a time series $X = x_i, i = 1, ..., m$ with m as the number of time series data, the chosen order of permutation n defines the dimension in phase space. For example, an order of permutation $n = 4$ defines a three-dimensional phase space and quantifies the rank order pattern of $x_i, x_{i+\tau}, x_{i+2\tau}, x_{i+3\tau}$. The relative frequency of each permutation is calculated as

$$p_j = \frac{z_j}{\sum z_k} \tag{11}$$

where z_j is the count of realization of the jth permutation, and z_k is the total realizations. Following the definition of Shannon entropy, the permutation entropy is defined as

$$H_p = -\sum_{j=1}^{n!} p_j \log_2(p_j) \tag{12}$$

The permutation entropy H_p is then normalized by the maximum permutation entropy $\log_2 n!$ following Domen's approach [16] noted as H_n as in Eq. (13), so that $H_n = 0$ corresponds to a monotonic relationship that is completely deterministic and $H_n = 1$ corresponds to randomness

$$H_n = \frac{-\sum_{j=1}^{n!} p_j \log_2(p_j)}{\log_2 n!} \tag{13}$$

An graphic example of data discretization for the calculation of permutation entropy is given in Fig. 9. A detailed step-by-step description is provided in Ref. [14]. Comparing to binning discretization for the symbol statistics and the modified Shannon entropy, the discretization approach for permutation represents the ranking order value in data sequence. This is the major difference between the definition of the permutation entropy and the modified Shannon entropy [3].

4.2 Diagnostic of Determinism With Varying Operating Conditions. The modified Shannon entropy and the permutation entropy of CA50 of HCCI and multicylinder SI combustion were calculated. These analyses are now extended to handle variations in engine operating conditions, which will be encountered given the transient nature of engine applications. The CA50 values are calculated from in-cylinder pressure with the three fast computational methods as well as the baseline dHR analysis. The influence of the three fast computational methods on entropies is examined.

For each of the four cylinders, 298 cycles of CA50 of an SI combustion engine are arranged by the firing order 1-3-4-2. To represent the entropy characterization of both random and deterministic data, 3000 cycles of HCCI CA50 are shown as a reference. The normalized permutation entropy H_n and the modified Shannon entropy with partition $N = 4$ and $L = 3$ of CA50 of HCCI and SI combustion are shown in Fig. 10(*c*). The order of permutation entropy n is chosen as 4. The time delay τ is chosen as 1 and window size $\hat{m}$ as 100. The procedure for calculating Shannon entropy is summarized below with 3000 cycles of HCCI data as an example. The same procedure applies to the permutation entropy.

- *Step 1*: Define the window of interest with size of $\hat{m}$ that contains $X = x_i, i = 1, ..., \hat{m}$ cycles. For $\hat{m} = 100$, 100 cycles are used to calculate the Shannon entropy H_s.
- *Step 2*: Slide the window of interest with a step of 1 cycle and repeat step 1 until cycle $x_{m-\hat{m}}$.

The window size $\hat{m}$ should be chosen considering the cycles required for the entropy to converge and will be studied in our future work.

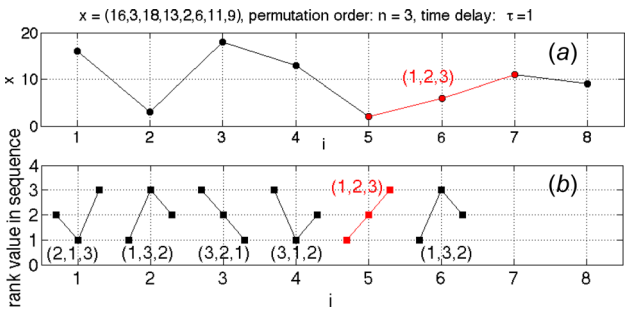

Fig. 9 Example of discretization of the calculation of permutation entropy: (*a*) time series example and (*b*) rank order

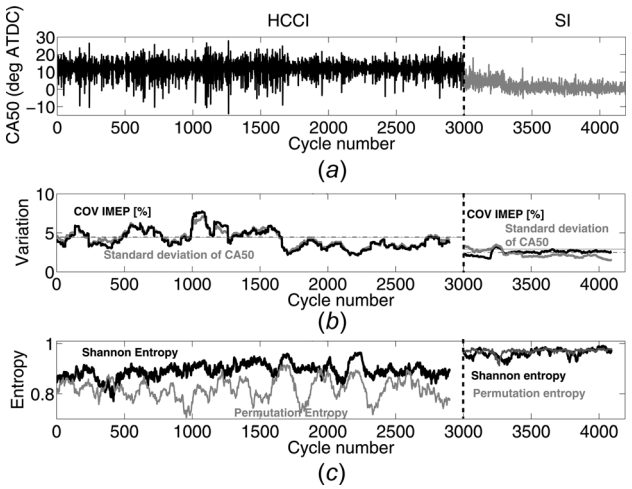

Fig. 10 Diagnostic of determinism in HCCI and SI combustion: (*a*) scatter plot of CA50 of HCCI and SI combustion, (*b*) COV of IMEP and standard deviation of CA50 for 100 cycles with step of 1, and (*c*) the modified Shannon entropy and the permutation entropy for 100 cycles with step of 1 cycle, the permutation order is 4

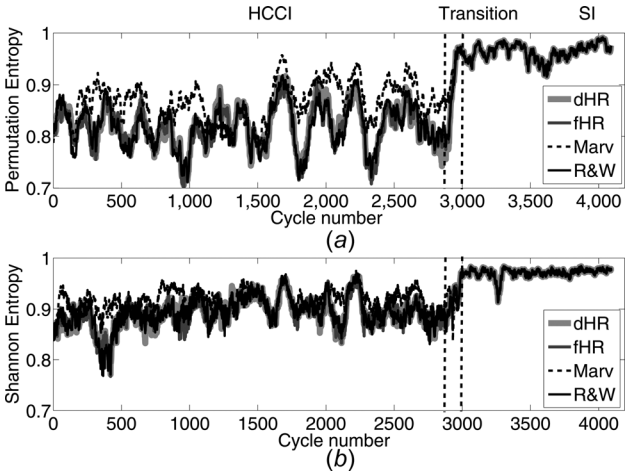

Fig. 12 Diagnostic of determinism in HCCI and SI combustion: (*a*) permutation entropy and (*b*) Shannon entropy. Note that 2999 cycles of HCCI combustion and 1192 cycles of SI combustion are artificially joined together for this analysis, which is intended to demonstrate the entropy's response to a change in operating conditions with no real experiment with combustion mode switch.

A graphic schematic of the sliding window method used to enable entropy calculation with varying operating conditions is shown in Fig. 11.

A scatter plot of the CA50 of HCCI and SI combustion calculated with dHR analysis is shown in Fig. 10(*a*) with HCCI data shown in black and SI data shown in gray. The difference in CA50 magnitude reflects the mean value difference without indication on determinism or randomness nature. Figure 10(*b*) provides quantification on the deviation from the covariance (COV) of indicated mean effective pressure (IMEP) and standard deviation of CA50, which are calculated within 100 cycles and move at the time lag of one cycle. SI combustion shows less deviation from the value calculated over the entire range of sampling cycles while HCCI combustion displays more intense fluctuations. Also, the standard deviation of CA50 and COV of IMEP correlates well. The entropy values deviate from one, suggesting the data to be deterministic in the HCCI region and approach one in the random SI region.

It should be mentioned that a discontinuity is observed in the temporal evolution of variations and entropies from around 2900–3000 for HCCI and after around 4100 for SI. The discontinuity range is determined by the chosen window size, which is 100 in the current result shown in Fig. 10. This is due to the artificially stitched HCCI and SI data, which does not represent a real experiment with observed abrupt switching between two combustion modes.

The influence of the three fast computational methods on entropy tracking is examined as follows. The permutation entropy and the modified Shannon entropy described above are calculated for CA50 from the three fast computational methods. Unlike Figs. 10(*b*) and 10(*c*), that the entropy evolutions are calculated separately for the HCCI and SI cycles, Fig. 12 shows calculations for the evolution of the entropies for artificially constructed 3000 cycles of HCCI connected by 298×4 cycles of SI combustion. This is to examine the entropy response to a known changed magnitude of determinism in the time series data. The permutation entropy is shown in Fig. 12(*a*), and the modified Shannon entropy is shown in Fig. 12(*b*).

For both permutation entropy and the modified Shannon entropy, the entropy evolutions of CA50 from fHR and R&W method agree well with the baseline CA50 from dHR. Marvin's method could result in an increase in both entropies, suggesting a decrease in the quantified determinism, consistent with the results of symbol statistics. Thus, Marvin's method should be avoided in the studies of CV.

To show the entropy response to a known changed magnitude of determinism in time series data, Fig. 12 is magnified between cycles 2900 and 3000 shown in Fig. 13. Both entropies gradually increase from lower values of deterministic HCCI to higher values of random SI cycles.

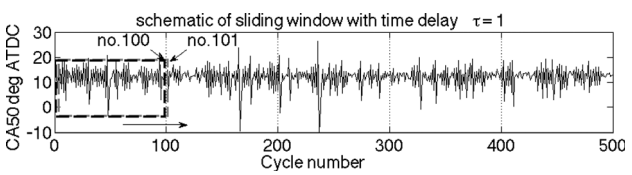

Fig. 11 Schematic of the sliding window used to enable entropy calculations with varying operating conditions

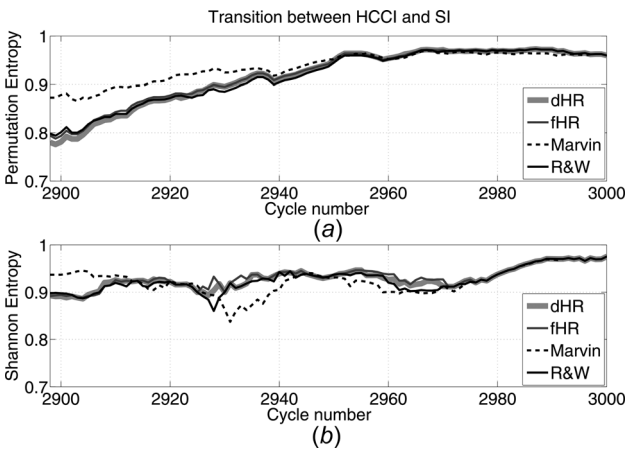

Fig. 13 Diagnostic of determinism in HCCI and SI combustion between HCCI and SI transition: (*a*) permutation entropy and (*b*) Shannon entropy. Note that 2999 cycles of HCCI combustion and 1192 cycles of SI combustion are artificially joined together for this analysis, which is intended to demonstrate the entropy's response to a change in operating conditions with no real experiment with combustion mode switch.

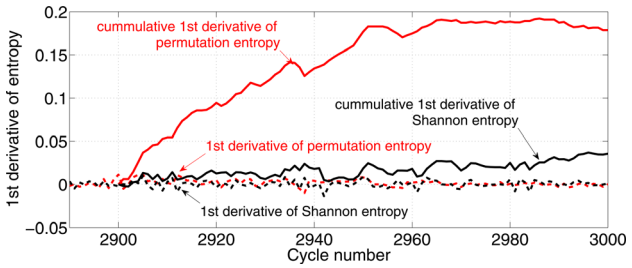

Fig. 14 The first derivative of permutation entropy and Shannon entropy with combustion phasing calculated from dHR analysis. Note that 2999 cycles of HCCI combustion and 1192 cycles of SI combustion are artificially joined together for this analysis, which is intended to demonstrate the entropy's response to a change in operating conditions with no real experiment with combustion mode switch.

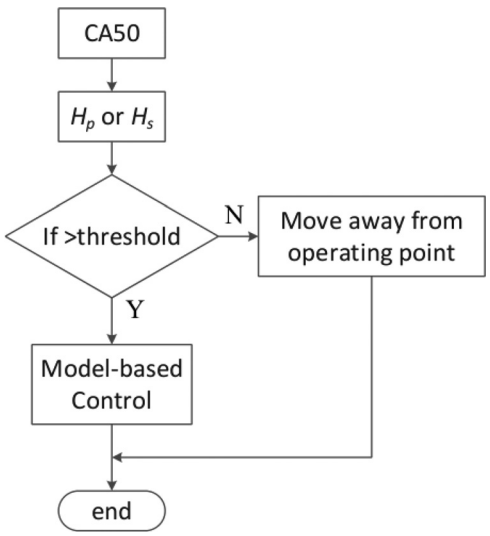

Fig. 15 Block diagram of selection of control strategy

To further examine the response of the two entropies, the first derivative and its cumulative value of the permutation entropy and Shannon entropy during the transition cycles 2900–3000 are shown in Fig. 14. Both entropies respond fast to the switch. The difference is that the magnitude of the permutation entropy is lower than the Shannon entropy, which might be advantageous when determining the threshold shown in Fig. 15 during the selection of the corresponding control strategy.

The entropy diagnostic method could assist in the selection of the corresponding control strategy. This process is illustrated as a diagram in Fig. 15. In the case of high CV with underlying deterministic patterns, it is possible to apply closed-loop combustion control on a cyclic-basis with a fixed mean value, such as injection timing in HCCI or spark timing in SI, to contract the CV. In the case of a random distribution, the high CV can be avoided by shifting operating conditions away from the unstable region. It should be noted that the threshold for both entropies will possibly need calibration. We intend to examine the threshold online on an engine dyno and present more results in our future publications. The determination of the value of the thresholds requires more thorough investigations and is beyond the current scope of this paper.

5 Conclusion

In summary, the current work has evaluated the affect that various fast CA50 calculation methods have on the quantification of CV as either random or deterministic. We have found that combustion phasing derived from the single-zone fHR and the R&W method had negligible impact when quantifying deterministic patterns, however, Marvin's method could cause certain deviations in the deterministic patterns that one should be aware of when quantifying CV. The robustness in quantifying the cyclic variability with on-board combustion phasing estimation indicates the potential for short-term online feedback control.

We have used a diagnostic method to quantify the deterministic and random nature of SI and HCCI combustion based on the permutation entropy, with its performance compared to modified Shannon entropy [3].

Combustion phasing derived from the single-zone fHR and the R&W method had negligible impact on the entropy tracking algorithms. However, the combustion phasing calculated from Marvin's method could increase both the permutation and the modified Shannon entropy, resulting in misinterpretation of the determinism of time series data.

Parameterization for the modified Shannon entropy and the permutation entropy is one of the interesting directions of future works that would extend the application of this quantification technique.

Nomenclature

A = combustion chamber surface area
A/F = air fuel ratio
CA50 = crank angle of 50% mass fraction burned
c_v = constant volume specific heat
h = heat transfer coefficient
H_n = normalized permutation entropy
H_p = permutation entropy
H_s = modified Shannon entropy
M = molar mass
m_c = in-cylinder charge mass
n = polytropic coefficient
P = pressure
p_k = probability of a sequence
Q_{apparent} = apparent heat release
Q_{ch} = chemical energy
Q_{ht} = heat transfer
Q_{hv} = lower heating value of the fuel
R = universal gas constant
T = temperature
T_w = cylinder wall temperature
V = volume
x_b = mass fraction burned
γ = polytropic exponent
θ = crank angle degree
ω = crank angle degrees per unit time

Subscripts

b = burned
f = property at end of combustion
u = unburned
σ = property at start of combustion

References

[1] Heywood, J., 1988, *Internal Combustion Engine Fundamentals*, 1st ed., McGraw-Hill, New York.
[2] Wagner, R., Edwards, K., Daw, C., Green, J., and Bunting, B., 2006, "On the Nature of Cyclic Dispersion in Spark Assisted HCCI Combustion," SAE Technical Paper No. 2006-01-0418.
[3] Sen, A., Litak, G., Edwards, K., Finney, C., Daw, C., and Wagner, R., 2011, "Characteristics of Cyclic Heat Release Variability in the Transition From Spark Ignition to HCCI in a Gasoline Engine," Appl. Energy, **88**(5), pp. 1649–1655.
[4] Larimore, J., Jade, S., Hellström, E., Stefanopoulou, A., Vanier, J., and Jiang, L., 2013, "Online Adaptive Residual Mass Estimation in a Multicylinder Recompression HCCI Engine," ASME Paper No. DSCC2013-3984.

[5] Nüesch, S., Hellström, E., Jiang, L., and Stefanopoulou, A. G., 2014, "Mode Switches Among SI, SACI, and HCCI Combustion and Their Influence on Drive Cycle Fuel Economy," American Control Conference (ACC), Portland, OR, June 4–6, pp. 849–854.
[6] Marvin, C., 1927, "Combustion Time in the Engine Cylinder and Its Effect on Engine Performance," NACA Report No. 276.
[7] Prakash, N., Martz, J., and Stefanopoulou, A., 2015, "A Phenomenological Model for Predicting Combustion Phasing and Variability of Spark Assisted Compression Ignition (SACI) Engines," ASME Paper No. DSCC2015-9883.
[8] Hellström, E., Stefanopoulou, A., and Jiang, L., 2013, "A Linear Least-Squares Algorithm for Double-Wiebe Functions Applied to Spark-Assisted Compression Ignition," ASME J. Eng. Gas Turbines Power, **136**(9), p. 091514.
[9] Hellström, E., Larimore, J., Stefanopoulou, A., Sterniak, J., and Jiang, L., 2012, "Quantifying Cyclic Variability in a Multi-Cylinder HCCI Engine With High Residuals," ASME J. Eng. Gas Turbines Power, **134**(11), p. 112803.
[10] Rassweiler, G., and Withrow, L., 1938, "Motion Pictures of Engine Flame Correlated With Pressure Cards," SAE Technical Paper 380139.
[11] Larimore, J., Hellström, E., Jade, S., Stefanopoulou, A., and Jiang, L., 2014, "Real-Time Internal Residual Mass Estimation for Combustion With High Cyclic Variability," Int. J. Engine Res., **163**(4), pp. 474–484.
[12] Hellström, E., Larimore, J., Jade, S., Stefanopoulou, A., and Jiang, L., 2014, "Reducing Cyclic Variability While Regulating Combustion Phasing in a Four-Cylinder HCCI Engine," IEEE Trans. Control Syst., **22**(3), pp. 1190–1197.
[13] Bandt, C., and Pompe, B., 2002, "Permutation Entropy: A Natural Complexity Measure for Time Series," Phys. Rev. Lett., **88**(17), p. 174102.
[14] Riedl, M., Muller, A., and Wessel, N., 2013, "Practical Considerations of Permutation entropy," Eur. Phys. J.: Spec. Top., **222**(2), pp. 249–262.
[15] Gotoda, H., Michigami, K., Ikeda, K., and Miyano, T., 2010, "Chaotic Oscillation in Diffusion Flame Induced by Radiative Heat Loss," Combust. Theory Modell., **14**(4), pp. 479–493.
[16] Domen, S., Gotoda, H., Kuriyama, T., Okuno, Y., and Tachibana, S., 2015, "Detection and Prevention of Blowout in a Lean Premixed Gas-Turbine Model Combustor Using the Concept of Dynamical System Theory," Proc. Combust. Inst., **35**(3), pp. 3245–3253.